Available online at www.sciencedirect.com
ScienceDirect
Journal of Nuclear Materials 376 (2008) 88–97
journal of nuclear materials
www.elsevier.com/locate/jnucmat

Fuel performance evaluation of rock-like oxide fuels

N. Nitani [a,b,*], K. Kuramoto [b], Y. Nakano [b], T. Yamashita [b], Y. Kimura [b], Y. Nihei [b], T. Ogawa [b]

[a] Chiba University, 1-33 Yayoi-cho, Inage-ku, Chiba 263-8522, Japan
[b] Japan Atomic Energy Agency, Tokai, Ibaraki 319-1195, Japan

Received 2 September 2007; accepted 19 January 2008

Abstract

The concept of the rock-like oxide (ROX) fuel has been developed for the annihilation of excess plutonium in light water reactors. Irradiation tests and post-irradiation examinations were carried out on candidate ROX fuels. The ternary fuel of YSZ–spinel–corundum system, the single-phase fuels of YSZ, the particle-dispersed fuels of YSZ in spinel or corundum matrix, and the blended fuels of YSZ and spinel or corundum matrix were fabricated and submitted to irradiation testings. The fuels containing spinel showed chemical instabilities with the vaporization of MgO component, which caused fuel restructuring. The swelling behavior was improved with the particle-dispersed fuels. However, the particle-dispersed fuels showed higher fractional gas release (FGR) than blended type fuels. The FGR of YSZ single-phase fuels were comparable to what would be expected for UO_2 fuel at the similar fuel temperatures. The YSZ single-phase fuel showed the best irradiation performance among the ROX fuels investigated.

PACS: 25.85.Ec

1. Introduction

The concept of the rock-like oxide (ROX) fuel has been developed for the annihilation of excess plutonium in the light water reactors (LWRs). Aims of adopting the ROX–LWR system are the nearly complete burning of plutonium and the direct disposal of spent ROX fuels without reprocessing [1,2]. The direct disposal of spent ROX fuels requires that the spent fuels must have high chemical stabilities under the geological conditions. The fluorite (yttria-stabilized zirconia; YSZ), spinel ($MgAl_2O_4$) and corundum (Al_2O_3) were initially selected as the candidate of ROX fuel matrices by the survey of properties of minerals and ceramics, which have high chemical and physical stabilities and low neutron capture cross-sections.

YSZ immobilizes plutonium, other actinides, and lanthanide fission-products (FPs) by making a series of solid solutions. However, its thermal conductivity is a little too low compared with the UO_2 and MOX fuels. The difference of the thermal conductivity of UO_2 and YSZ becomes smaller as the temperature is increased. The thermal conductivity of YSZ is about two thirds of that of UO_2 at 1000 K [3].

The thermal conductivity of YSZ can be improved by combining it with spinel or corundum, which has a higher thermal conductivity. We have shown that the YSZ composite containing about 50 mol% $MgAl_2O_4$ and 15 mol% UO_2 showed higher thermal conductivity than UO_2, in the temperature range from room temperature to 1700 K [3]. However, it is known that the corundum matrix fuels show larger irradiation swelling [4]. On the other hand, the resistance of spinel to neutron irradiation is high [5], but that to fission fragment damage might not be sufficient.

* Corresponding author. Address: Japan Atomic Energy Agency, Tokai, Ibaraki 319-1195, Japan. Tel.: +81 29 282 6380; fax: +81 29 282 6122.
E-mail address: shirasu.noriko@jaea.go.jp (N. Nitani).

0022-3115/$ - see front matter © 2008 Elsevier B.V. All rights reserved.
doi:10.1016/j.jnucmat.2008.01.019

We have proposed dispersion of coarse particles of actinides-containing phase in spinel or corundum matrix [2,6], because it is preferable to localize fission fragments damage to a small region of the matrix to suppress the extensive swelling and the degradation of thermal conductivity.

Little was known about the in-pile irradiation behavior of these ceramic matrices. In order to obtain information on the irradiation behavior of ROX fuels, we performed irradiation tests and post-irradiation examinations of the candidate ROX fuels for three times.

The primary objective of the first irradiation test was the confirmation of FP behavior. The fuels with 10 mol% Pu were prepared to produce sufficient amount of FP elements. The amount of Pu was twice of that assumed for the ROX fuel burning in LWR system, resulting in higher power density. Because of the restrictions on the total amount of Pu in the irradiation rig, the small disk-shaped samples were used.

The aim of the second and the third irradiation tests was to evaluate the fuel integrity, particularly to confirm the performance of particle-dispersed fuels. The pellet fuels with 20% enriched uranium was used. To study the effect of the fuel particle size, two types of composite fuel were prepared, the particle-dispersed type (YSZ inclusion size of 250 μm) and blended type (YSZ inclusion size of 10–50 μm). The YSZ single-phase fuel was also fabricated for the comparison.

This paper summarizes the irradiation behavior of ROX fuels in the three irradiation tests, and evaluates their performance. Recently, irradiation tests on inert matrix fuels (IMF) have been carried out by several groups, with the object to study the transmutation of americium and/or the incineration of plutonium [7–9]. The comparison is also made with the results of the latter IMF irradiation experiments.

2. Experimental

2.1. Samples

The samples are summarized in Table 1. In all samples, either uranium or plutonium was incorporated in the YSZ phase, forming solid solutions.

The ternary system of YSZ–spinel–corundum (SCB) fuel was used for the first irradiation test. The SCB fuels were small disks of about 3 mm in diameter and 1 mm in height, in which Pu with 94% ^{239}Pu was added into the YSZ phase.

For the second irradiation test, five types of fuels were prepared; the particle-dispersed fuels with spinel or corundum matrix (SD1, CD1), the blended fuels with either spinel or corundum matrix (SB, CB), and the single-phase fuels of YSZ (Z1). For the third irradiation test, three types of fuels were prepared; the particle-dispersed fuels with spinel or corundum matrix (SD2, CD2), and the single-phase fuels of YSZ (Z2). The samples for the second and the third tests were pellets of about 5.4 mm in diameter and 5.6 mm in height, in which 20% enriched U was used as surrogate of Pu. On the third irradiation test, the Z2, SD2, and CD2 fuels were designed to make the volumetric number density of fissile atom equal in all fuels. The fabrication process of each fuel is described in detail elsewhere [6,10,11].

2.2. Irradiation

The fuels were irradiated in JRR-3. The irradiation conditions are summarized in Table 2. The arrangements of irradiation capsules are described in Refs. [10,11]. The linear power was estimated from the activity measurement of fluence monitors. For the second and third irradiation

Table 1
The compositions, dimensions and densities of the fuels

Fuel[a]	Fuel type	YSZ inclusion size (μm)	Composition (mol%)					Dimension (mm)		Fissile density (cm^{-3})	Density (%TD[c])
			YSZ[b]	PuO_2	UO_2	$MgAl_2O_4$	Al_2O_3	Diameter	Height		
1st irradiation test (Pu-ROX)											
SCB	YSZ blended in spinel–corundum matrix	2–10	16.7	11.1	–	11.1	61.1	3	1	2.11×10^{21}	81.6
2nd irradiation test (U-ROX1)											
Z1	YSZ solid solution		81.75	–	18.25	–	–	5.5	5.6	9.72×10^{20}	85.7
SD1	YSZ particles with spinel matrix	250	21.88	–	36.23	41.89	–	5.4	5.5	1.37×10^{21}	90.6
CD1	YSZ particles with corundum matrix	250	18.12	–	30.01		51.87	5.5	5.5	1.39×10^{21}	93.1
SB	YSZ blended in spinel matrix	10–50	21.88	–	36.23	41.89	–	5.4	5.7	1.37×10^{21}	91.3
CB	YSZ blended in corundum matrix	10–50	18.12	–	30.01	–	51.87	5.4	5.7	1.39×10^{21}	90.6
3rd irradiation test (U-ROX2)											
Z2	YSZ solid solution		78.00	–	22.00	–	–	5.3	5.7	1.16×10^{21}	92.0
SD2	YSZ particles with spinel matrix	100–200	33.35	–	29.65	37.00	–	5.2	5.7	1.16×10^{21}	93.2
CD2	YSZ particles with corundum matrix	100–200	27.70	–	24.63	–	47.67	5.2	5.7	1.16×10^{21}	92.9

[a] The notation of fuels was changed form previous papers to make it more intelligible.
[b] YSZ: 78.6 mol% ZrO_2 + 21.4 mol% $YO_{1.5}$.
[c] TD: theoretical density.

Table 2
Estimated irradiation conditions and burnups of the fuels

Irradiation	Pu-ROX disk		
Fuel	SCB-1	SCB-2	SCB-3
	Average/maximum		
Volumetric power (GW m^{-3})	1.97/2.30	2.45/2.81	1.90/2.10
Disk temperature (K)	1040 ± 50	1270 ± 10	980 ± 50
Irradiation time (days)	97	97	97
Volumetric burnup (GW d m^{-3})	192	237	184

Irradiation	U-ROX1 pellet					U-ROX2 pellet		
Fuel	Z1	SD1	CD1	SB	CB	Z2	SD2	CD2
	Average/maximum					*Average/maximum*		
Linear power (kW m^{-1})	13.9/15.2	23.0/25.4	24.9/27.9	23.4/26.0	20.7/22.7	18.7/27.7	16.5/23.3	16.3/22.8
Volumetric power (GW m^{-3})	0.60/0.65	1.05/1.10	1.05/1.18	1.04/1.15	0.90/0.99	0.77/1.14	0.68/0.96	0.67/0.94
T surface of pellet (K)	990/1030	1250/1310	1300/1360	1440/1510	1290/1350	800/960	760/890	770/890
T center of pellet (K)	1490/1580	1740/1850	1820/1930	1940/2080	1730/1830	1490/1960	1060/1360	1020/1350
Irradiation time (days)	100	100	100	100	100	280	280	280
Volumetric burnup (GW d m^{-3})	59	100	105	103	88	275	248	245

tests, the pellets were placed inside the stainless steel cladding with helium at ambient pressure. The surface and center temperatures of the fuel pellets were estimated from the linear powers and the measured surface temperatures of cladding. The burnups were calculated using the SRAC95 code system [12].

The power density of SCB fuel in the first test was very high. Nevertheless, the fuel temperature was not so high, due to the small and thin dimension of fuels. In the second irradiation test, the irradiation temperature of SD1, SB, CD1 and CB fuels was significantly higher than that of normal conditions in LWRs. The higher temperatures of these samples are due to the inadequate heat removal in this particular irradiation capsule, while the linear power rate was set comparable to the LWR fuels. On the other hand, the irradiation temperature of Z1 fuel was much lower than the other fuels, because of lower fissile densities and lower neutron flux. The irradiation condition of the third test was closer to normal conditions in LWR regarding the temperature. Also the differences of linear powers and burnups among the fuels were small.

2.3. Post-irradiation examination

The pellets stack was examined by X-ray radiography. The precise diameters of the fuel pins were measured from four directions at 45° intervals using an electronic micrometer. The swelling of pellets was evaluated from the changes in the fuel stack lengths and the pellet diameters. Diameter change of the pellet was evaluated from the initial pellet diameter, a gap between the pellet and cladding, and profilometry value.

Gases in the fuel pin were collected and analyzed by the puncture test; the isotopic abundance of Kr and Xe were measured by the mass spectrometry. The fractional gas release (FGR) was obtained from the measured Xe and Kr volume and calculated total yield of Xe and Kr. Total yield and isotopic abundance of Kr and Xe were obtained from the burnup calculation using the SRAC95 code.

The fuel pellets were examined by X-ray diffraction analysis (XRD), ceramography, scanning electron microscopy (SEM) and electron probe microanalysis (EPMA). XRD was carried out at two points; the center region of fuel pellet, and the periphery region. A collimator with 1mm diameter and a receiving slit with 0.6 mm were used for XRD.

3. Results

3.1. Dimensional stability

SCB fuel disks hardly kept the original shapes; some had large cracks and the others were broken into small pieces. Though the apparent volume increase was observed by a low magnification telescope, it was impossible to determine precise sizes of the irradiated disks. Rough measurements indicated about 11% increase in diameter.

Although the cracks were formed in the pellets in the second and the third irradiation tests, there were no significant fragmentations. The radial gaps between pellet and cladding and the axial gaps between pellets were also maintained.

No stack elongation was observed for all fuel pin within the experimental error of 0.1 mm. The profilometry of each pin showed that the diameter expansion was very small, less than 10 μm, except for the SB target where diameter increase of 60 μm was recorded at the maximum value. Radial and volumetric swellings of pellets are summarized in Table 3. Since the axial dimensional change was not observed for all pellets, the volumetric swelling is simply determined by radial dimensional change. The second test revealed that the blended fuels (SB, CB) showed larger swelling than the particle-dispersed fuels (SD1, CD1) and the YSZ single-phase fuel (Z1).

Table 3
Swelling, measured and calculated FP gas volume and FP gas release rate of the ROX fuels

Fuels		SCB-1	SCB-2	SCB-3	Z1	SD1	CD1	SB	CB	Z2	SD2	CD2
Diameter increase (%)		–	–	10.8	2.0	2.7	2.1	5.0	2.8	2.8	3.6	2.3
Volume increase (%)		–	–	–	<4.0	5.5	4.3	10.2	5.7	5.6	7.2	4.7
Measured volume of released FP gas (cm^3)	Kr	0.009	0.008	0.006	0.004	0.08	0.05	0.05	0.016	0.06	0.41	0.87
	Xe	0.157	0.146	0.112	0.021	0.60	0.36	0.36	0.11	0.42	3.04	6.46
Xe/Kr ratio		17.3	17.9	18.0	5.4	7.5	7.2	7.2	7.0	7.0	7.4	7.4
Calculated volume of produced FP gas (cm^3)	Kr	0.012	0.013	0.010	0.131	0.219	0.234	0.229	0.199	1.14	1.01	1.00
	Xe	0.215	0.241	0.177	0.946	1.57	1.68	1.65	1.42	8.38	7.38	7.35
Xe/Kr ratio		18.2	18.3	18.1	7.1	7.2	7.1	7.2	7.2	7.4	7.3	7.3
FP gas release rate (%)		73	61	63	2.4	38	22	22	8	5	41	88

3.2. Fission-gas release

The FGR values are listed in Table 3. The released Xe/Kr gas ratios were measured to be 7.0–7.5 and 17.3–18.0 for pellet shape fuels and disk shape fuels, respectively, which agreed well with the theoretical values, 7.1–7.4 and 18.1–18.3. Difference in the Xe/Kr ratio between the disk-type and pellet-type fuels is due to the difference in the fissile nuclides; mainly ^{239}Pu for the disk-type fuels, and ^{235}U for the pellet-type fuels. The smaller Xe/Kr ratio of the Z1 fuel is considered due to errors associated with a very small amount of gas in the measurement.

Contrary to the swelling behavior, the FGR of particle-dispersed fuels was larger than that of the blended fuels. It should be noted that the corundum-based CD2 fuel, which was irradiated at about 1000 K, showed extremely high FGR. The YSZ single-phase fuels (Z1, Z2) showed much lower FGR than the other fuels.

3.3. X-ray diffraction

Four types of phases were identified on the SCB fuels by XRD analysis; fluorite-type phase, hibonite, corundum, and spinel. The amount of hibonite phase ($M^{3+}Al_{11}O_{18}$ and/or $M^{3+}MgAl_{11}O_{19}$) increased by the irradiation.

The XRD patterns of the center and the surface region of SD2 fuel pellets are shown in Fig. 1, with the XRD patterns on an as-fabricated sample. The estimated irradiation temperatures were about 1000 K and 800 K for the center and periphery region, respectively. Three kinds of phases; fluorite, spinel, and small amount of corundum phase were detected. Fluorite appeared to be separated into two phases for the center region of the SD2 fuel pellet, though its cause is not identified yet.

Corundum is known to suffer amorphization by irradiation at lower temperatures [13]. The XRD patterns of the irradiated CD2 fuel clearly showed the existence of

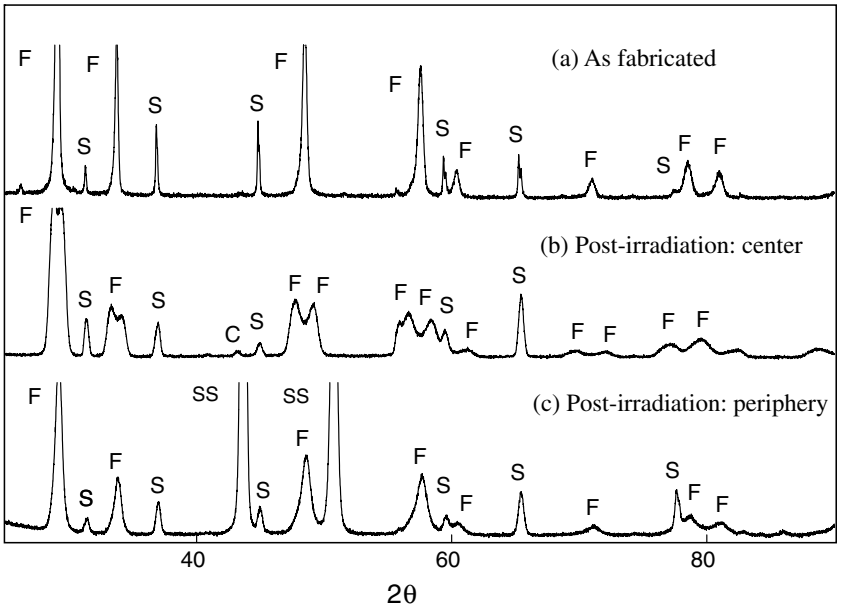

Fig. 1. X-ray diffraction patterns of SD2 fuel. (a) As-fabricated; (b) post-irradiation, the center region of fuel pellet; (c) post-irradiation, the surface region of fuel pellet; S: spinel phase, F: fluorite phase, C: corundum phase, SS: cladding.

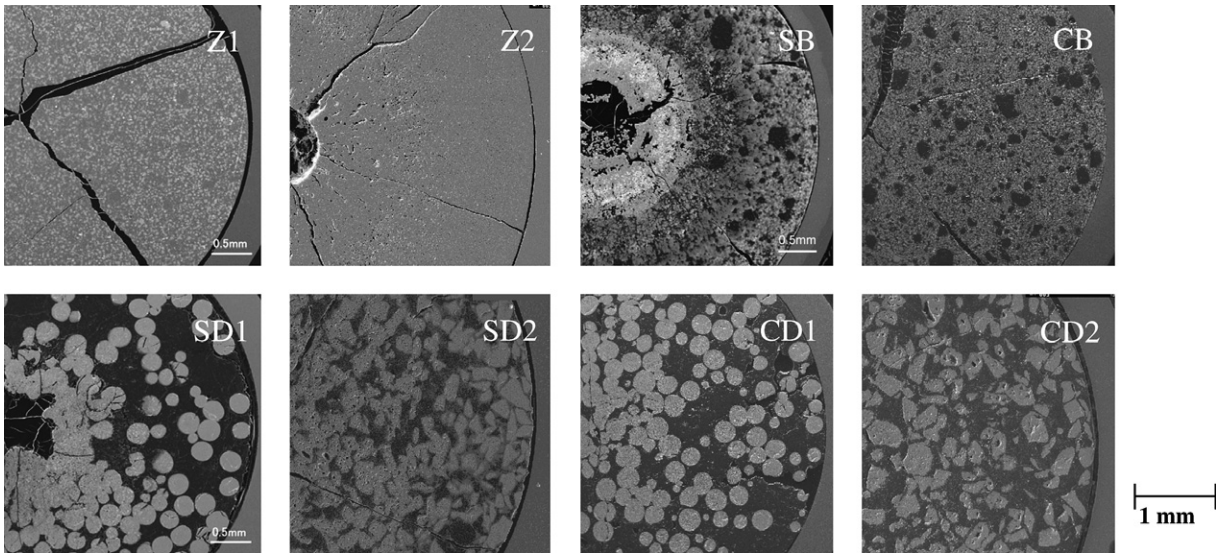

Fig. 2. The SEM images of ROX fuels [14,17].

crystalline corundum phase, and there was little indication of amorphization.

In the XRD pattern of Z2 fuel, the peaks slightly broadened, but no additional peaks were observed.

3.4. Microstructure

In the SCB fuel, the hibonite phase was already formed in as-fabricated fuels. At the last step of the fuel preparation, fuel disks were sintered at 1670 K in 8% H_2/Ar atmosphere and some Pu^{4+} were reduced to Pu^{3+} to form the Pu-hibonite ($PuMgAl_{11}O_{19}$) [10]. By irradiation of the fuels, a large fraction of Pu moved from the fluorite phase to the hibonite phase, especially at high irradiation temperatures and lower oxygen potentials [10].

The cross-sectional appearances of the fuels of second and third irradiation tests are shown in Fig. 2, and the line profiles of U, Zr, Al, and Mg for the SB are shown in Fig. 3 with the SEM image. Restructuring and central-hole formation were observed in the SD1 and SB fuel, which have spinel matrix. These fuel pellets comprised roughly three regions; the center region consisted only of YSZ; the middle region of YSZ and corundum; the outer region of the original YSZ and spinel [14,15]. MgO was detected on the inner surface of cladding tube. Thus, the spinel-based fuel irradiated at such high centerline temperatures around 2000 K showed decomposition and restructuring. The equilibrium vapor pressure of Mg (g) on spinel is high under a low oxygen potential, analogously to that on MgO [16]. The vapor pressure of Mg (g) is about four orders of magnitude higher than that of Al (g). The high irradiation temperature, the large temperature gradient, and the low oxygen potential caused the vaporization of MgO component and subsequent spinel decomposition. MgO condensed on the cladding inner surface. By comparing the pellet cross-section and the temperature distribution, it is

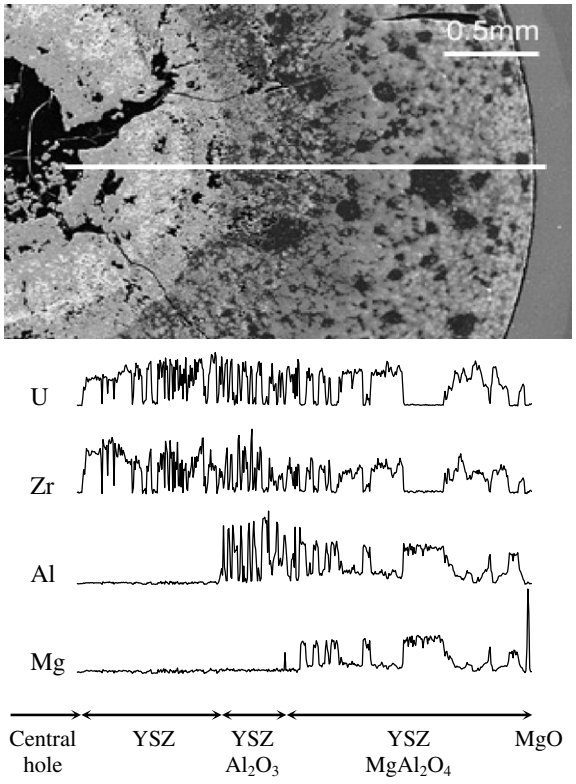

Fig. 3. The line profiles of U, Zr, Al, and Mg and SEM image corresponds to the position measurement for SB fuel. White line shows the analyzed position [15].

judged that the vaporization of MgO component occurred at temperatures exceeding about 1700 K [15]. The restructuring of fuel pellet was not observed in the spinel-based fuel (SD2) irradiated below 1400 K [17]. It was found that there is a temperature limit on use of spinel-based fuel.

By modifying the assembly design of ROX and addition of Er burnable poison, the total power peaking factor could be reduced to as low as 1.7 [18], that is small enough

to keep the fuel temperature lower than 1700 K, when the average linear heat rate of 18 kW m^{-1} is assumed [18]. In that ROX–PWR core, it is possible to suppress the maximum linear heat rate to 31 kW m^{-1}.

On the other hand, the aggregation of the YSZ particles and the restructuring were rarely observed for the all corundum-based (CD1, CB and CD2) fuels. Regardless of irradiation temperatures, the fuel pellets showed uniform structure throughout the pellet cross-section [17].

No appreciable changes were found in the Z1 fuel which irradiated at low temperature and with low power. On the other hand, several radial cracks and a central-hole of less than 0.8 mm diameter were observed in the Z2 fuel. The central-hole was presumably caused by migration of pores [17].

4. Discussion

The results of ROX and other IMF irradiation experiments are summarized in Table 4. The comparison in view of the pertinent irradiation behavior is made as follows.

4.1. Swelling

The SCB fuels showed remarkable large swelling, about 11% increase in diameter notwithstanding rather low irradiation temperature. The behavior of the YSZ, spinel and corundum phases may be inferred from the other irradiation tests, but that of hibonite can be only inferred from the first test with SCB fuels. The fraction of hibonite phase increased by the reaction with fission-product lanthanide elements, and by the movement of the plutonium from the fluorite to the hibonite phase. Volume increases by conversion of corundum to hibonite (about 3%) [10]. The fission-gas bubble growth would be also enhanced by the phase change.

The hibonite should have also suffered fission fragment damages directly, since a large fraction of plutonium existed in this phase. The volumetric power density (2–3 GW/m^3) was much higher than the maximum LWR fuel conditions by a factor of 3–4. The irradiation behavior of hibonite itself, however, has not been clarified yet.

The particle-dispersed fuels (SD1, CD1) showed lower swelling than the blended fuels (SB, CB). It was thus confirmed that the swelling behavior was suppressed by the control of the YSZ particle size. The SB fuel showed the largest swelling. Marked swelling of spinel-based fuel was also observed in the irradiation by Georgenthum et al. [19] where a fuel with micro-dispersed UO_2 inclusions in spinel matrix was studied. Furthermore, in OTTO experiment [20,21], a fuel pin with micro-dispersion of

Table 4
An overview of the results of ROX and other IMF irradiation experiments

	Fuel	Type[a]	Fis. density (g/cm^3)	Max. linear power (kW m^{-1})	Max. fuel temp. (K)	Burnup (kW d cm^{-3})	FIMA (%)	FGR (%)	Swelling (%)	Ref.
ROX										
Z1	$(U,Zr,Y)O_2$	s	0.40	15.2	1580	59	3.7	2.4	<4.0	This work
Z2	$(U,Zr,Y)O_2$	s	0.48	27.7	1960	275	12.0	5.0	5.6	This work
SD1	$(U,Zr,Y)O_2$	mad	0.56	25.4	1850	100	4.1	38	5.5	This work
SD2	$(U,Zr,Y)O_2$	mad	0.48	23.3	1360	248	10.8	41	7.2	This work
SB	$(U,Zr,Y)O_2$	mid	0.56	26.0	2080	103	4.2	22	10.2	This work
CD1	$(U,Zr,Y)O_2$	mad	0.57	27.9	1930	105	4.2	22	4.3	This work
CD2	$(U,Zr,Y)O_2$	mad	0.48	22.8	1350	245	10.7	88	4.7	This work
CB	$(U,Zr,Y)O_2$	mid	0.57	22.7	1830	88	3.6	8	5.7	This work
IFA-651										
	$(Er,Y,Pu,Zr)O_2$	s	0.75	38.9	2175	217	–	18	–	[20]
	$(Er,Y,Pu,Zr)O_2$	s	0.75	34.1	1945[b]	315	–	32	–	[20]
	$(Er,Y,Pu,Zr)O_2$	s	0.60	32.2	2285	278	–	34	–	[20]
OTTO										
	$(Er,Y,Pu,Zr)O_2$	s	0.37	19.8	1790	176	–	9.2	–	[20,21]
	$(Y,Pu,U,Zr)O_2$	s	0.34	20.0	1775	178	–	6.1	0.2 ± 0.6[c]	[20,21]
	$(Er,Y,Pu,Zr)O_2$	mid	0.32	15.6	1075	144	–	0.1	2.7 ± 0.6[c]	[20,21]
	$(Y,Pu,U,Zr)O_2$	mid	0.31	15.2	1040	136	–	–	5.1 ± 0.6[c]	[20,21]
	$(Er,Y,Pu,Zr)O_2$	mad	0.31	15.0	1135	142	–	4.3	1.0 ± 0.6[c]	[20,21]
	$(Y,Pu,U,Zr)O_2$	mad	0.30	14.8	1085	133	–	6	1.3 ± 0.6[c]	[20,21]
EFFTRA-T3										
	UO_2	mid	0.047	5.1	–	–	19.1	0.1	-0.8 ± 1	[22]
	UO_2	mad	0.049	5.6	–	–	19.7	43	6.5 ± 5.0	[22]
EFTTRA-T4ter										
	UO_2	mid	0.19	–	–	–	32.0	–	10.9 ± 1.5	[22]

[a] s = single-phase fuel; mid = micro-dispersion of IMF particles <25 μm in $MgAl_2O_4$ (Al_2O_3 for CB in ROX); mad = macro-dispersion of IMF particles 200–250 μm in $MgAl_2O_4$(Al_2O_3 for CD1, CD2 in ROX).
[b] Calculated for a pellet with central-hole.
[c] Axial swelling.

$(Zr,Y,U,Pu)O_2$ particles (<25 μm) in spinel matrix failed during irradiation, because of a high radial swelling. Klaassen et al. reported that the sample with 25 wt% UO_2 in spinel (EFTTRA-T4ter) showed a significant swelling, 11 vol.%; on the other hand, the sample with lower content (7.3 wt%) of UO_2 in spinel (EFTTRA-T3) did not show any appreciable swelling [22]. Wiss and Matzke [23] have shown that the spinel exhibited a large swelling when irradiated with 72 MeV iodine ions to a fluence of 10^{16} ions cm^{-2}. Swelling as high as 15% was observed for ion irradiations at 773 K and about 7% at 1173 K. At 1473 K, no measurable swelling was observed. These facts suggested that the swelling of spinel was mainly caused by fission fragment damage.

It is known that the neutron resistance of corundum is inferior to that of spinel [5], and corundum becomes amorphous by fission damage. Berman et al. reported that the fuel specimen irradiated at low temperature (about 560 K) showed a large swelling (about 30%) due to amorphization of the corundum phase [4]. In this work, the swelling of the corundum-based fuels was substantial but not so large as that of spinel. It is considered that the irradiation temperature was high enough to anneal the damage. XRD analysis of the irradiated fuels clearly showed the existence of a crystalline corundum phase, with little indication of amorphization, at irradiation temperatures of 800–1000 K [17].

The YSZ single-phase fuels (Z1, Z2) showed low swelling rates. OTTO experiment has also shown that the axial swelling of YSZ single-phase fuels was comparable with that of MOX fuel (1.7 ± 0.6%) [21].

4.2. Fractional fission-gas release

Although the SCB disk fuels showed high FGR, it is not easy to compare their FGR with those of the other fuel types due to very high power density and fragmentation of the disks.

The FGR of the Z2 fuel is about 5%, in spite of a central-hole formation, high irradiation temperature, and substantial burnup. Though the linear power of Z2 fuel irradiation was comparable to conventional UO_2 fuel, its irradiation temperature was higher, due to lower thermal conductivity.

For UO_2 fuel, Vitanza et al. reported that the threshold temperature for onset of appreciable gas release (>1%) becomes lower with increasing burnup [24]. The so-called Vitanza limit is shown in Fig. 4. The UO_2 burnups are shown as number of fissions per unit volume to compare with the YSZ fuels in this study. The top axis shows the burnups corresponding to the fission density, for UO_2 fuel. The data are also compared with that on UO_2 fuel by Kamimura et al. [25] in Fig. 4.

The Z2 fuel showed similar level of the FP gas release with UO_2 fuel at similar volumetric fission density and temperature. Streit et al. investigated the irradiation behavior of YSZ based fuel (IMF-ATT in IFA-651) [8]. The FGR also found to be comparable to what would be expected

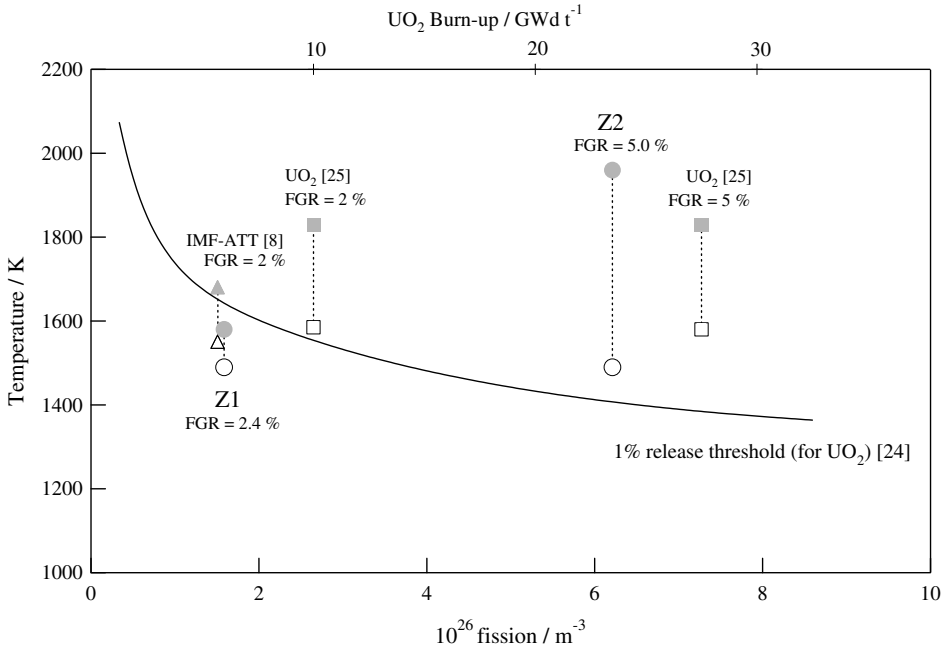

Fig. 4. The comparison of the FGR behavior between UO_2 fuel and YSZ single-phase fuels. The relations between irradiation temperature and burnp are shown. The line shows the Vitanza limit that describes the temperature and burnup threshold above which more than 1% of the fission-gas is released in UO_2 fuel. The top axis shows the UO_2 burn-ups corresponding to the fission density, for UO_2 fuel. Circle: this study, Square: UO_2 by Kamimura et al. [25], triangle: IMF-ATT fuel ($(Er,Y,Pu,Zr)O_2$ system) in IFA-651 experiment [8]. Solid and open marks indicate maximum and average temperatures, respectively.

for UO_2 fuel at these fuel temperatures. The FGR of Z1 fuel was relatively higher, which may be caused by the lower density of fresh Z1 pellet, (~86% TD).

Degueldre et al. found that the Xe diffusion coefficient in YSZ is much lower than that of UO_2 [26]. Strong retention of implanted Xe in YSZ was observed up to 1773 K. However, the FGR of YSZ based inert matrix fuels was comparable to that of UO_2. Degueldre et al. considered that the smaller Xe diffusion constant of YSZ is due to a smaller solubility of Xe. The solubility of Xe in YSZ might be increased by the addition of UO_2 or PuO_2. Furthermore, significant grain growth was observed for IMF-ATT fuel [8]. Hence, the grain boundary movement would be also a factor determining FGR in the YSZ single-phase fuels.

The composite fuels showed higher FGR than YSZ single-phase fuels. The open paths of micro-crack in the single-phase fuel are harder to form than that in the particle-dispersed fuels: the FP gases tended to be confined in grain boundaries in the former. Another factor to be considered is that the fissile content of YSZ phase for single-phase fuel was lower than those for the particle-dispersed fuels to realize the same level of heavy metal loading. For example, the mole fraction of U in YSZ phase was 47.1 mol% for SD2 and CD2 fuel, and 22.0 mol% for Z2 fuel. This difference would have resulted in the difference in various irradiation-induced processes.

Contrary to the swelling behavior, the FGR of particle-dispersed fuels (SD1, CD1), was larger than that of the blended fuels (SB, CB). The high FGR values suggest that the FP gas release is not driven by atomistic diffusion through matrices but by transport through open path provided by minute cracks. Minute cracks may occur by the stresses caused from a thermal expansion difference between the large YSZ fuel particles and matrices. The thermal expansion coefficients of spinel and YSZ (containing UO_2) are 8.5×10^{-6} and $1.1 \times 10^{-5}\ K^{-1}$, respectively, at 298–1273 K [3]. A similar FGR behavior was observed in EFTTRA-T3 experiment [27,28]. The FGR of dispersed type fuel with large fissile inclusions (150 μm) was remarkably higher than that with small fissile inclusions (<1 μm) dispersed type fuel, and many cracks were observed in the matrix of large fissile inclusions dispersed type fuel.

The FGR of the CD2 fuel was extremely high. That was about twice higher than the SD2 fuel. Since the YSZ particles for the SD2 and CD2 fuels were almost identical, and the irradiation conditions were almost the same, the difference in behavior is linked to the difference in the properties of the matrices. The FGR of the CD1 and CB fuels, which were irradiated at higher temperatures, are not so high as that of the CD2 fuel. It is apparently against simple expectation. The irradiation temperature of the CD2 fuel that showed remarkably high FGR was much lower than those of the CD1 and CB fuels as shown in Table 3. The thermal stresses between YSZ particles and matrices would become larger by increasing the temperature, and the stress caused the hair crack generation. Furthermore, FP gases have higher diffusion rates in higher temperature condition.

It is expected that the annealing of the irradiation damage is a function of temperature. White et al. reported the crystallization mechanism and kinetics of amorphous Al_2O_3 [29]. The crystallization kinetics is closely related to temperature. The speed of transformation at 1233 K is about a hundred times faster than that at 1073 K [29]. The irradiation temperature of CD2 fuel was close to the recovery temperature of amorphous Al_2O_3, about 1073–1173 K [13,29]. Though the amorphization was not found for the CD2 fuels from XRD pattern, the damage annealing in corundum phase would have been less in CD2 than in CD1 and CB fuels. The much slower damage annealing would be responsible to the extremely high FGR of CD2 fuel.

4.3. Comparison and evaluation of the ROX fuel

The fuels of YSZ–$MgAl_2O_4$–Al_2O_3 ternary system showed large swelling and high fission-gas release rate. The phase changes such as newly hibonite formation with trivalent actinide and lanthanide causes a few complications, such as increased swelling and FGR. Besides, the melting temperature becomes lower by forming ternary eutectic compounds, than eutectic temperature of YSZ–$MgAl_2O_4$ system. Though the eutectic temperature of YSZ–$MgAl_2O_4$ was about 2200 K [3], the eutectic temperature of YSZ–$MgAl_2O_4$-Al_2O_3 system was about 2000 K. Considering these effects, the system that contains the excess Al_2O_3 is undesirable.

The hibonite of $LnAl_{11}O_{18}$ type compounds (Ln = lanthanides) were meta-stable and they could be stabilized by the introduction of divalent cations in the crystal lattice, $LnMgAl_{11}O_{19}$ [30]. For the corundum-based fuels, the amount of the hibonite phase was small. It might be due to the fact that uranium surrogated plutonium in these samples. However, almost all fission-product lanthanides existed in fluorite phase as identified by EPMA in the corundum-based fuels. It is assumed that the hibonite phase is more easily formed under the condition of existence of Mg. In the spinel-based fuels, the hibonite phase formation was hardly observed, where the restructuring was not observed.

The blended type fuels (micro-dispersed type fuels) showed lower FGR. In OTTO and EFTTRA experiments, the micro-dispersed type fuels showed very low FGR, whereas the SB fuel in this study showed high FGR. The vaporization of MgO component, spinel decomposition and restructuring enhanced the gas release from SB fuel. On the other hand, the blended type fuels showed large swelling. For micro-dispersed fuel in OTTO experiment, the cladding was failed during irradiation, because of high radial swelling. The large volumetric swelling is the major disadvantage of the spinel-based fuel. The spinel-based fuel irradiated at about 2000 K showed the vaporization of MgO component and subsequent restructuring. It was confirmed that the appreciable restructuring was avoidable by lowering the irradiation temperature.

Table 5
Comparison of irradiation behaviors of ROX fuels

Fuel type	Swelling	FGR	Pellet integrity
YSZ–spinel–corundum system	–	–	–
	Very large	Very high	Fragmentation
YSZ–spinel system			
Particle-dispersed type			
Irradiated at about 2000 K	+	–	–
	Substantial but not decisive	High	Vaporization of MgO component and restructuring (>1700 K)
Irradiated below 1400 K	+	–	+
	Substantial but not decisive	High	Some crack and gas bubble formation
Blended type	–	–	–
	Over 10 vol.%	High	Vaporization of MgO component and restructuring (>1700 K)
YSZ–corundum system			
Particle-dispersed type			
Irradiated at about 2000 K	+	–	+
	Substantial but not decisive	High	Some crack and gas bubble formation
Irradiated below 1400 K	+	–	+
	Substantial but not decisive	Extremely high	Some crack and gas bubble formation
Blended type	+	–	+
	Substantial but not decisive	Slightly high	Some crack and gas bubble formation
YSZ single-phase system	+	+	–
	Substantial but not decisive	Low, the behavior was analogous to UO_2	Crack formation and densification

The serious swelling behavior was improved by making the fissile particle size lager. On the other hand, the particle-dispersed type fuels showed high FGR than blended type fuels. The significantly high FGR on macro-dispersed fuel were also observed in EFTTRA-T3 experiment. However, the FGR of the macro-dispersed fuel in OTTO project was almost similar to the single-phase fuel, due to better fuel fabrication (sphere fuel inclusion shape and appropriate density) and irradiation condition of low power density (max. linear power ~15 kW m^{-1}). Optimization of the density of fuel constituent (matrix and fuel particle) and a gap width between fuel particles and matrix will be the key for the improvement of performance of the particle-dispersed fuel. There would be a room for improving the FGR reduction for particle-dispersed fuel. The linear power of EFTTRA-T3 experiment was lower than that of OTTO, however, the fuel showed very high FGR. The fissile inclusion of EFTTRA-T3 was not diluted with YSZ. Not only fission-gas concentration in the particles became higher, but also the thermal expansion coefficient of UO_2 is higher than YSZ [3], which resulted in the lager thermal stress.

The corundum-based fuels irradiated at sufficiently high temperature did not show the significant appearance changes such as swelling and heterogeneity of fuel structures. The fatal drawback was not observed on corundum in the high temperature irradiation. However, the corundum-based fuel irradiated at lower temperatures corresponding to the recovery temperature of amorphous Al_2O_3 showed extremely high FGR.

The YSZ single-phase fuels showed low FGR and small swelling behavior. Though the irradiation temperature of YSZ single-phase fuel was high, the YSZ single-phase fuel showed best irradiation behavior among the ROX fuels subjected to the present tests. The FGR of YSZ single-phase fuel was comparable to that of UO_2.

The results of irradiation behavior of ROX fuels are summarized in Table 5, in order to facilitate the comparison.

5. Conclusions

To evaluate the irradiation behavior of ROX fuels, the irradiation tests and the post-irradiation examinations were carried out.

The spinel-based particle-dispersed type fuels were irradiated successfully, and showed relatively good irradiation behavior. The thermal conductivities were improved by combined use of YSZ with spinel, and the swelling behaviors were reduced by enlarging the fuel particle size. On the other hand, the particle-dispersed fuel showed high FGR. Further improvements on fabrication technologies are necessary for use of particle-dispersed fuel.

The chemical and irradiation instability were revealed for spinel. The vaporization of MgO component and restructuring occurred at the area of over about 1700 K. Thus, there are severe restrictions on the use of spinel-based fuel. By modifying the assembly design of ROX and addition of Er burnable poison, the total power peaking factor could be reduced to as low as 1.7 [18], that is small enough to keep the fuel temperature less than 1700 K, when the average linear heat rate of 18 kW m^{-1} is assumed [18].

The YSZ single-phase fuel showed good irradiation stability. The irradiation temperature of YSZ single-phase fuel

was high, due to the low thermal conductivity of YSZ. Nevertheless the YSZ single-phase fuel showed good irradiation behavior; low FGR and small swelling. The estimated fuel center temperature rises to about 2500 K, under the condition of a conventional PWR [31]. The temperature seems sufficiently lower than the melting point (3000 K) [3], but it would be necessary to reduce the linear heat rate to lower the fuel temperature than that of conventional UO_2 fuel, when using YSZ single-phase fuel. Engineering remedies would be to suppress the power peaking of the reactor core as mentioned above, or using the annular pellets.

The Pu transmutation rate of the modified ROX–LWR core is 80–85%. It is extremely higher than that of MOX fuel (25–32%) [18]. It is worthwhile to have further argument and investigation on the ROX–LWR system, the high Pu transmutation and its direct disposal.

References

[1] H. Akie, T. Muromura, H. Takano, S. Matsuura, Nucl. Technol. 107 (1994) 182.
[2] T. Yamashita, K. Kuramoto, H. Akie, Y. Nakano, N. Nitani, T. Nakamura, K. Kusagaya, T. Ohmichi, J. Nucl. Sci. Technol. 39 (2002) 865.
[3] N. Nitani, T. Yamashita, T. Matsuda, S. Kobayashi, T. Ohmichi, J. Nucl. Mater. 274 (1999) 15.
[4] R.M. Berman, M.L. Bleiberg, W. Yeniscavich, J. Nucl. Mater. 2 (1960) 129.
[5] R.J.M. Konings, K. Bakker, J.G. Boshoven, R. Conrad, H. Hein, J. Nucl. Mater. 254 (1998) 135.
[6] T. Shiratori, T. Yamashita, T. Ohmichi, A. Yasuda, K. Watarumi, J. Nucl. Mater. 274 (1999) 40.
[7] D. Warin, R. Conrad, D. Haas, G. Heusener, P. Martin, R.J.M. Konings, R.P.C. Schram, G. Vambenepe, in: Proceedings of International Conference on Back-end of the Fuel Cycle: From Research to Solutions (Global-2001), Paris, France, 11–14 September 2001, p. 204.
[8] M. Streit, W. Wiesenack, T. Tverberg, Ch. Hellwig, B.C. Oberlander, J. Nucl. Mater. 352 (2006) 349.
[9] R.P.C. Schram, R.R. van der Laan, F.C. Klaassen, K. Bakker, T. Yamashita, F. Ingold, J. Nucl. Mater. 319 (2003) 118.
[10] T. Yamashita, N. Nitani, H. Kanazawa, M. Magara, T. Ohmichi, H. Takano, T. Muromura, J. Nucl. Mater. 274 (1999) 98.
[11] N. Nitani, K. Kuramoto, T. Yamashita, K. Ichise, K. Ono, Y. Nihei, J. Nucl. Mater. 352 (2006) 365.
[12] K. Okumura, K. Kaneko, K. Tsuchihashi, JAERI-Data/Code, 96-015, 1996 (in Japanese).
[13] S. Furuno, N. Sasajima, K. Hojou, K. Izui, H. Otsu, T. Muromura, T. Matsui, Nucl. Instrum. and Meth. B 127&128 (1997) 181.
[14] N. Nitani, K. Kuramoto, T. Yamashita, Y. Nihei, Y. Kimura, J. Nucl. Mater. 319 (2003) 102.
[15] N. Nitani, K. Kuramoto, T. Yamashita, Y. Nakano, H. Akie, in: Proceeding of International Conference on Back-end of the Fuel Cycle: From Research to Solutions (Global-2001), Paris, France, 11–14 September 2001, p. 018.
[16] T. Sasamoto, H. Hara, T. Sata, Bull. Chem. Soc. Jpn. 54 (1981) 3327.
[17] N. Nitani, K. Kuramoto, Y. Nakano, T. Yamashita, T. Ogawa, in: Proceedings of 15th International Conference on Nuclear Engineering (ICONE15) Nagoya, Japan, 22–26 April 2007, p. 10183.
[18] H. Akie, Y. Sugo, R. Okawa, J. Nucl. Mater. 319 (2003) 166.
[19] V. Georgenthm, J. Brillaud, N. Chauvin, N. Pelletier, J. Noirot, D. Plancq, Progr. Nucl. Energy 38 (2001) 317.
[20] Ch. Hellwig, M. Streit, P. Blair, T. Tverberg, F.C. Klaassen, R.P.C. Schram, F. Vettraino, T. Yamashita, J. Nucl. Mater. 352 (2006) 291.
[21] G.J.L.M. de Haas, F. Klaassen, R. Schram, G. Dassel, R. Schuring, Ch. Hellwig, T. Yamashita, HOTLAB European Hot Laboratories Research Capacities and Needs Plenary Meeting 2004, Halden, Norway, 6–8 September 2004.
[22] F.C. Klaassen, R.P.C. Schram, K. Bakker, E.A.C. Neeft, R. Conrad, R.J.M. Konings, Actinide and Fission Product Partitioning and Transmutation, Paris, France, Organisation for Economic Co-Operation and Development, Nuclear Energy Agency, 2003, p. 549.
[23] T. Wiss, Hj. Matzke, Radiat. Meas. 31 (1999) 507.
[24] C. Vitanza, E. Kolstad, U. Graziani, in: Proceedings of ANS Topical Meeting on LWR Fuel Performance, Portland, 1979.
[25] J. Kamimura, K. Ohira, K. Okubo, N. Itagaki, in: Proceedings of International Meeting on LWR Fuel Performance, Salamanca, Spain, 22–26 October 2006, p. 5.
[26] C. Degueldre, M. Pouchon, M. Dobeli, K. Sickafus, K. Hojou, G. Ledergerber, S. Abolhassani-Dadras, J. Nucl. Mater. 352 (2001) 115.
[27] K. Bakker, R. Belvroy, F.A. van den Berg, et al., Progr. Nucl. Energy 38 (2001) 313.
[28] E.A.C. Neeft, K. Bakker, H.A. Buurveld, et al., Progr. Nucl. Energy 38 (2001) 427.
[29] C.W. White, L.A. Boatner, P.S. Sklad, C.J. McHargue, J. Rankin, G.C. Farlow, M.J. Aziz, Nucl. Instrum. and Meth. B 32 (1988) 11.
[30] M. Gasperin, M.C. Saine, A. Kahn, F. Laville, A.M. Lejus, J. Solid State Chem. 54 (1984) 61.
[31] H. Akie, H. Takano, Y. Anoda, J. Nucl. Mater. 274 (1999) 139.